Talanta 76 (2008) 1058–1064

Contents lists available at ScienceDirect

Talanta

journal homepage: www.elsevier.com/locate/talanta

Facile synthesis of hollow Co_3O_4 microspheres and its use as a rapid responsive CL sensor of combustible gases

Fei Teng[a,b,*], Wenqing Yao[b], Youfei Zheng[a], Yutao Ma[c], Tongguang Xu[b], Guizhi Gao[a], Shuhui Liang[b], Yang Teng[d], Yongfa Zhu[b,*]

[a] Department of Chemistry, Nanjing University of Information Science & Technology, Nanjing 210044, PR China
[b] Department of Chemistry, Tsinghua University, Beijing 100084, PR China
[c] School of Science, Beijing Jiaotong University, Beijing 100044, PR China
[d] Department of Information Science, Suzhou Institute of Trade & Commerce, PR China

ARTICLE INFO

Article history:
Received 3 February 2008
Received in revised form 27 April 2008
Accepted 5 May 2008
Available online 18 May 2008

Keywords:
Hollow Co_3O_4 microspheres
Chemiluminescence
CO oxidation
Gas sensor

ABSTRACT

The hollow Co_3O_4 microspheres (HCMs) were prepared by the carbonaceous templates, which did not need the surface pretreatment. The chemiluminescence (CL) and catalytic properties for CO oxidation over these hollow samples were evaluated. The samples were characterized by scanning electron microscopy (SEM), energy disperse spectra (EDS), transmission electron microscopy (TEM), selected area electron diffraction (ED), X-ray diffraction (XRD), temperature-programmed desorption (TPD) and N_2 adsorption. The influences of filter' band length, flow rate of gas, test temperature, and particle structure on CL intensities were mainly investigated. It was found that compared with the solid Co_3O_4 particles (SCPs), HCMs had a stronger CL intensity, which was ascribed to its hollow structure; and that CL properties of the catalysts were well correlated with their reaction activities. Moreover, HCMs were used to fabricate a highly sensitive gas detector, which is a rapid and effective method for the selection of catalysts or the detection of environmental deleterious gases.

© 2008 Elsevier B.V. All rights reserved.

1. Introduction

In 1976, Breysse et al. [1] first reported chemiluminescence (CL) phenomenon. They observed that a weak catalytic luminescence phenomenon occurred while CO was catalytically oxidized on the ThO_2 surface. This luminescence mode was defined as "cataluminescence". Since the 1990s, micro- and nano-particles have been widely applied in various fields of catalysis [2], chemical and biochemical sensing [3], and biological imaging [4]. Many investigations have indicated that CL property of nanoparticles would be promising for new applications [5]. Recently, Zhu et al. [6] investigated CL of organic vapor over different nanoparticles, including MgO, TiO_2, Al_2O_3, Y_2O_3, $LaCoO_3$:Sr^{2+} and $SrCO_3$. Rakow and Suslick [7] reported that the nanoparticles are potentially suitable for processing as a chip-mounted sensor array. Nakagawa et al. [8] have manufactured a γ-Al_2O_3 sensor to detect ethanol, acetone and butyric acid, which utilize the combustibility of these chemicals on this solid. Okabayashi et al. [9] have also manufactured a Dy-doped γ-Al_2O_3 sensor used for hydrocarbon gases. Zhang and co-workers [10–12] have designed the highly selective CL sensors for ammonia, hydrogen sulfide and acetone. They reported that ZrO_2 nanoparticles-based sensor for ethanol has no response to hexane, cyclohexane, ethylene, hydrogen, ammonia and nitrogen oxides. While Tb was doped, the sensibility of Tb–ZrO_2 sensor can be enhanced as high two level as that of the undoped one. A lot of researches about CL properties of micro- or nano-particles have focused on CL applications in analysis [13]. Nevertheless, the highly sensitive CL sensors are still challenged by the structure properties of materials. It is well known that the properties of materials are strongly dependent on the morphology and structure of the particles. Compared with solid particles, the hollow structures generally have a higher surface area and a lighter weight. Hollow structures with nano- to micro-meters dimensions are an important class of materials, which are widely used in various fields, such as drug delivery carriers, light-weight structural materials, microreactors. Generally, the hollow particles are prepared by the templated methods. In order to form the coating, the surface modification of the templates is usually needed beforehand [14]. It is needed to develop a simple templated method to prepare the hollow spheres.

The spinel Co_3O_4 has great application potential in heterogeneous catalysts, anode materials in Li ion rechargeable batteries, solid-state sensors, solar energy absorbers, and so on. CO oxidation

* Corresponding author at: Department of Chemistry, Nanjing University of Information Science & Technology, Nanjing 210044, PR China; Department of Chemistry, Tsinghua University, Beijing 100084, PR China. Tel.:/Fax: +86 10 6278 7601.
E-mail addresses: tfwd@163.com (F. Teng), zhuyf@mail.tsinghua.edu.cn (Y. Zhu).

0039-9140/$ – see front matter © 2008 Elsevier B.V. All rights reserved.
doi:10.1016/j.talanta.2008.05.011

of Co_3O_4 has been extensively researched. Recently, hollow Co_3O_4 have been reported by the researcher [15,16]. To the best of our knowledge, nevertheless, fewer researches have reported the CL properties of gases over hollow Co_3O_4 and the essence correlations between CL process and catalytic reaction [17].

Herein, carbonaceous microspheres (CMs) were synthesized by a hydrothermal method; and hollow Co_3O_4 microspheres (HCMs) were prepared by the impregnation and annealing. The carbonaceous templates can be directly used to accept the foreign species to form a coating without surface modification. The CL and catalytic properties for CO oxidation over HCMs were evaluated, and the correlation between them was revealed. Most importantly, a highly sensitive CL sensor was fabricated by HCMs.

2. Experimental

2.1. Synthesis of the samples

All chemicals used in this experiment were analytical grade (Beijing Chemical Reagent Factory), and used as purchased.

2.1.1. Synthesis of carbonaceous microspheres

The carbonaceous templates were prepared by a hydrothermal method [18]. Typically, 5 g of glucose was dissolved in water (40 mL). The mixture was continuously sonicated for 5 min until a clear solution was formed. The solution was then transferred to a Teflon-lined stainless-steel autoclave with 50 mL capacity, and kept at 170 °C for 12 h. The black products were recovered by centrifugation. The solid was washed by water and alcohol at least four cycles of centrifugation/washing/redispersion, respectively. Finally, the product was dried at 80 °C overnight in an oven.

2.1.2. Synthesis of hollow Co_3O_4 microspheres

The hollow microspheres were prepared by impregnating the CMs with nitrate solution. Typically, 0.5 g of CMs was dispersed in 100 mL 1.0 M $Co(NO_3)_2$ solution under sonification. The mixture was continuously sonicated for 30 min at room temperature, and then magnetically stirred for 24 h, so that Co ions entered the surface layers of CMs; the solids were separated by centrifugation, and washed with water once; then the sample were dried in an oven at 80 °C overnight. To remove the carbonaceous templates, the sample was calcined at 450 °C for 2 h at a rate of 1 °C min^{-1} under flowing air.

2.1.3. Synthesis of the solid Co_3O_4 particles (SCPs)

The solid Co_3O_4 particles were obtained by a solid-state decomposition reaction of cobalt nitrate. The cobalt nitrate solids were ground homogeneously in mortar, and then calcined at 700 °C for 2 h in air.

2.2. Characterization

The samples were characterized by X-ray diffraction (XRD) on a Rigaku D/MAX-RB X-ray powder diffractometer, using graphite monochromatized Cu Kα radiation ($\lambda = 0.154$ nm), operating at 40 kV and 50 mA. The patterns were scanned from 10° to 70° (2θ) at a scanning rate of 5° min^{-1}. The morphology, surface microstructure and compositional distribution of the sample were determined by a JEOL JSM 6400 scanning electron microscope (SEM) equipped with a Link ISIS energy disperse spectra analyzer (EDS). The same instrument was involved in the recording of X-ray maps. The acceleration voltage in all cases was 15 keV and the current was 1.2 nA. In the recording of X-ray maps the current of 6.7 nA was used. The morphology and microstructure of the sample were also characterized with a transmission electron microscopy (TEM) (JEOL 200CX) with the accelerating voltage of 200 kV. The powders were dispersed in ethanol ultrasonically, and then the samples were deposited on a thin amorphous carbon film supported by copper grids. A nitrogen adsorption isotherm was performed at 77 K on a Micromeritics ASAP 2010 gas adsorption analyzer. Surface areas were calculated by the BET method. The sample was degassed at 250 °C for 3 h before the measurement.

2.3. Evaluation of chemiluminescence properties

The CL detection system employed in this work is shown in literature [6]. The detect system consists of a CL-based sensor, a digital programmable temperature controller of the sensor, and an optical detector. The CL sensor was made by sintering a 0.2-mm-thick layer of the catalyst powder on a cylindrical ceramic heater of 5 mm in diameter. Typically, 0.02 g of Co_3O_4 powders were mixed with absolute ethanol to prepare a paste, and the paste was coated on the surface of heating tube; and then, it was dried in an oven at 110 °C for 24 h and heated at 450 °C for 1 h in air to form a film. In order to accurately control the thickness, the same procedure was repeated for two times. The obtained sensor was set in a quartz tube of 12-mm (i.d.) through which an air at atmospheric pressure flows at a constant rate. A certain volume pulse of CO was injected into the airflow. The sample gas can flow only through the outside of the ceramic heater because this ceramic tube is solid. The temperature of the sensor was controlled by a digital temperature controller. The CL intensity at a certain wavelength was measured by a photon-counting method with a BPCL ultraweak chemiluminescence analyzer (BPCL, Chemiluminescence analyzer made by Biophysics Institute of the Chinese Academy of Science). In the experiment, the optical filter with the wavelength of 640 nm was used. Before each test, the catalyst sensor was heated at 450 °C for 1 h in air to avoid the influence of previous absorbates.

2.4. Evaluation of catalytic activity

The oxidation of CO was carried out in a conventional flow system at atmospheric pressure. 0.1 g of Co_3O_4 powders were loaded in a quartz reactor (inner diameter: 5 mm), with quartz beads packed at both ends of the catalyst bed. The thermal couple was placed in the catalyst bed to monitor the reaction temperature since CO oxidation is an exothermic reaction. Before each run, the catalyst was flushed with air (200 mL min^{-1}) at 450 °C for 1 h in order to remove the previous absorbates from the catalyst surface, and then cooled to 30 °C. A gas mixture of 1 vol.% CO and 99 vol.% air was fed to the catalyst bed at a certain flowing rate of 200 mL min^{-1}. The inlet and outlet gas compositions were analyzed by an on-line gas chromatograph with a GDX-403 GC-column (1.5 m × 4 mm) at 100 °C and a hydrogen flame ionization detector (FID).

3. Results and discussion

3.1. Formation of carbonaceous microspheres and hollow Co_3O_4 microspheres

Fig. 1 shows SEM and TEM images of CMs. It can be observed that CMs have uniformed size of about 5 μm. It seems that their surfaces are smooth (Fig. 1a); but the TEM image reveals that the surfaces of CMs are not smooth but coarse, and there exist surface layer (Fig. 1b). This can be ascribed to the removal of residual organic compounds (i.e. oligosaccharides). The surfaces of CMs became coarse due to the removal of these chemicals from the surface layer while CMs were washed with water and alcohol. Li and co-worker [18] have reported that there are some nanopores in the surface layer while they synthesized carbonaceous spheres. The existence

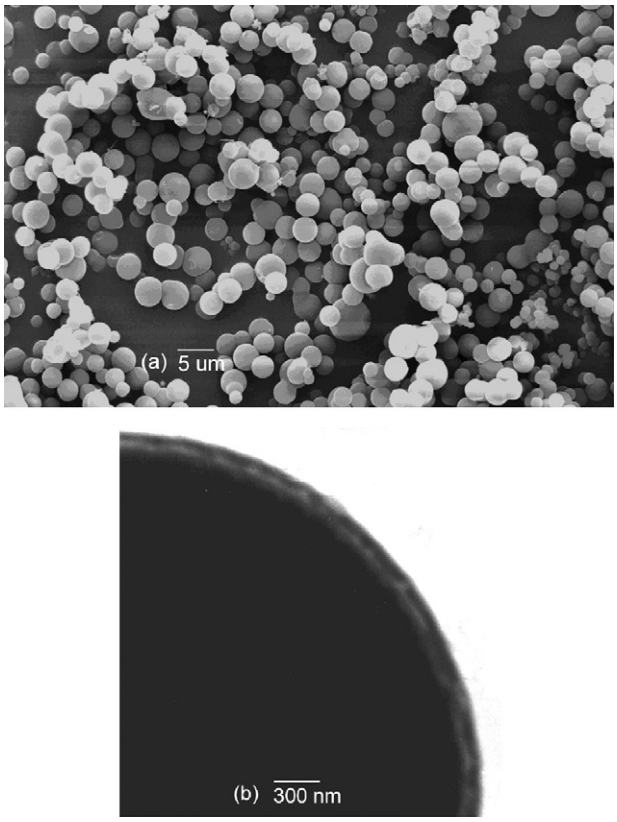

Fig. 1. SEM (a) and TEM micrographs (b) of carbonaceous microspheres (CMs).

of nanopores in surface layer is very important, which can not only increase the surface area, but also favor for the accommodation of foreign species.

Carbonaceous microspheres are formed by dehydration of saccharide under hydrothermal conditions [18–20]. It has been reported that under hydrothermal conditions, a variety of chemical reactions for glucose could take place, which resulted in a complex mixture of organic compounds. As a result, it is difficult to determine exactly the chemical reactions in the sealed autoclave. In the experiment, after hydrothermal treatment, the appearance of black solids and the increased viscosity of the resulting solution indicated that the aromatic compounds and oligosaccharides may have formed, which has been denoted a "polymerization" process [18–20]. The carbonization step may arise from the cross-linking process of oligosaccharides or other macromolecules. The formation of CMs seems to conform to the LaMer model [21]. While the solution reached a critical supersaturation, a short burst of nucleation occurred. The resulting nuclei then grew uniformly through the diffusion of solutes toward the nuclei surfaces until the final size was attained. Importantly, in comparison to the synthesis of polymer spheres, the adopted approach has two outstanding features: (i) the synthetic approach is very simple since no intricate operations are involved; (ii) the approach is environmentally friendly, since no toxic reagents were used. For preparation of polymer microspheres, however, toxic reagents (organic solvents, initiators or/and surfactants) are commonly used.

The surfaces of CMs are hydrophilic due to the functional groups (OH, C=O) [18–20] and the surface layer contains the nanopores [22]. This means that the templates can be directly used without needing surface treatment. We assumed that the surface layers of CMs could adsorb or accommodate cobalt ions. This may be through electrostatic or chelating interactions between foreign metal ions and surface functional groups (OH, C=O) [18–20]. Upon subsequent drying, a sol–gel process may be involved in the formation of cobalt oxide due to the formation of chelate compouds [23]. Further, the annealing treatment in air can not only remove the carbonaceous templates, but also give rise to the self-supporting cobalt oxide nanocrystals. Fig. 2(a and b) presents the typical SEM micrographs of HCMs. The sizes of HCMs are 2–3 μm, which are much smaller than those (5 μm) of the templates. It is obvious that HCMs retained the morphological characteristics of the original templates except for shrinkage in size (about 40%). It is easily understood that upon annealing, the dehydration and dehydroxylation may lead to the contraction of the sample. As a result, the rough surface coatings were constructed by randomly aggregated Co_3O_4 nanocrystals. Further, the surface microstructure of individual HCM was scanned by high-magnification SEM (Fig. 2c). HCMs have the hollow interiors of about 2.6 μm in size and the shells of about 200 nm in thickness. The HCMs have a coarse surface structure, which is different from that of CMs. In the process of annealing in air, the formation of Co_3O_4 and the combustion of templates occurred simultaneously. Co_3O_4 nanocrystals were formed and trapped within the carbonaceous networks; therefore, the nanocrystals could be effectively protected from growth or agglomeration. When the templates were removed, the Co_3O_4 nanocrystals formed the shells. The EDS spectra (Fig. S1 of supporting material) of HCMs firmly demonstrate that the sample consist of cobalt. HCMs were further characterized by TEM. As shown in Fig. 3(a and b), the clear–obscure contrast between the inner and the outer regions of the particles can be observed clearly, revealing the presence of hollow interior. electron diffraction (ED) patterns (Fig. 3c) of the sample further demonstrate that the shells consist of Co_3O_4 polycrystals. Fig. S2 (see supporting material) gives the TEM images of SCPs, which were prepared by decomposition of nitrate. The solid particles have the diameters of 100–200 nm and they agglomerated severely.

XRD patterns were performed to determine the structure of the samples. After being annealed at 450 °C, the sample was composed of Co_3O_4 nanocrystals (Fig. 4a). Co_3O_4 nanocrystals show a spinel structure with the lattice constants $a_0 = 0.8084$ nm (JCPDS file no. 43-1003: space group of Co_3O_4: $Fd3m$). Fig. 4b shows the XRD patterns of carbonaceous templates. The broad peak with low peak intensity centered at about $2\theta = 23.5°$ can be indexed as [0 0 2] diffraction peak of turbostratic and polyaromatic carbon. The broadening of the "graphite" peaks actually indicates the highly disordered structures [19]. While the sample was calcined in a muffle at 450 °C under flowing air, carbonaceous chemicals combusted to form CO_2. In this process, a significant amount of heat would be released. The local temperatures of the sample may be higher than 450 °C. Co (II) was partly oxidized to form Co (III). On the other hand, the functional groups (OH) can impart the reduction ability to Co (III), which can reduce metal ions into lower valence ion. Such reduction ability has been reported in literatures [24,25]. As a result, Co_3O_4 was formed. The XRD patterns of SCPs by decomposition of nitrate were also shown in Fig. S2 (supporting material). Calculated by Scherrer equation, the average crystal size is about 32.2 nm, which is larger than that (25.5 nm) of HCMs.

3.2. The CL properties over the samples

We have researched the effects of the filter's band length and flow rate of gas on CL intensity. These research results are given in Figs. S4 and S5 (supporting material). The result showed that the highest CL intensity was obtained with 640-nm filter (Fig. S4). The CL intensity increases with an increase of the flow rate and it saturates above a flow rate ($F = 200\ mL\ min^{-1}$) (Fig. S5). This may mean that the whole reaction is mainly controlled by a diffusion process at $F \leq 200\ mL\ min^{-1}$. At $F \geq 200\ mL\ min^{-1}$, the whole

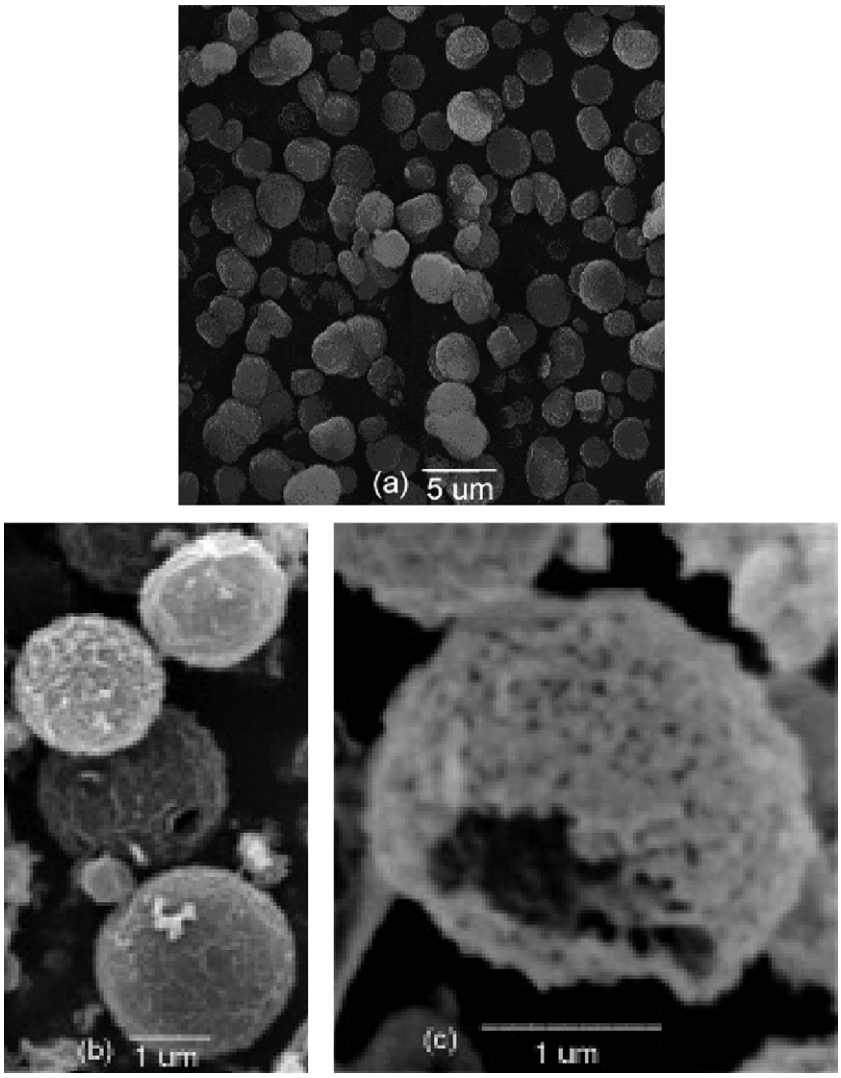

Fig. 2. SEM micrographs of hollow Co_3O_4 microspheres (HCMs): (a) low magnification images of HCMs; (b) broken HCMs; (c and d) high-resolution images of HCMs surface.

reaction is mainly controlled by a surface reaction. Therefore, the CL spectra were determined at $F = 200\,mL\,min^{-1}$ with the 640-nm filter in the latter experiments. Typically, Fig. 5 shows the effect of test temperature on the CL intensity of HCMs. The CL intensities increased from 6×10^3 to 7×10^4 a.u. while the temperature increased from 160 to 300 °C. It is clear that the test temperature has a significant influence on CL intensity. This is because CO conversion increased with the temperature. More CO molecules were oxidized into CO_2 molecules at high temperatures. It is important for CL determination to maintain a constant test temperature. The influence of CO concentration (C) on CL intensity of HCMs is shown in Fig. 6 and Table 1. A good linear correlation between CL intensity and CO concentration can be observed in the concentration range ($5.0–300.0\,\mu g\,mL^{-1}$), and the relative coefficient is 0.995. The detection limit of CL sensor for CO has been determined as low as $0.23\,\mu g\,mL^{-1}$. This means that CL properties of the catalyst should be determined at a constant concentration of CO.

Table 1
Analytical characteristics of CL determination for CO of hollow Co_3O_4 microspheres (HCMs)

Linear range, C ($\mu g\,mL^{-1}$)	5.0–320.0
Regression equation	$I^a = 67.8C + 55.2$
Relative coefficient	0.995
Detection limit ($\mu g\,mL^{-1}$)	0.23

[a] I, CL intensity; C, CO concentration.

Many researchers have proposed that the CL luminescence results from the excited species produced in catalytic oxidation [26,27]. The exothermal chemical reaction produces energy enough to induce the transition of an electron from its ground state to an excited electronic state. This electronic transition is often accompanied by vibrational and rotational changes in the molecule. CL is observed when the electronically excited product relaxes to its ground state with emission of photons [28]. CL reaction can be represented with the following formula:

$$CO_2(\text{ads.}) + \text{Energy} \rightarrow {}^*CO_2(\text{ads.}) \rightarrow CO_2 + h\nu \quad (1)$$

It is accepted that CO_2 was the luminescence species. While CO molecules were oxidized on the catalyst surface, an amount of energy was released, which would be absorbed by CO_2 molecules. As a result, CO_2 molecules would jump from ground state up to electronic excited state ($^*CO_2$). While the electronic excited $^*CO_2$ molecules decayed to the ground state, a CL was generated. CL spectra are closely correlated with the catalytic reaction, in which the conversion of CO into CO_2 is directly related to the catalytic properties of the catalysts. The easier the catalytic reaction was, the

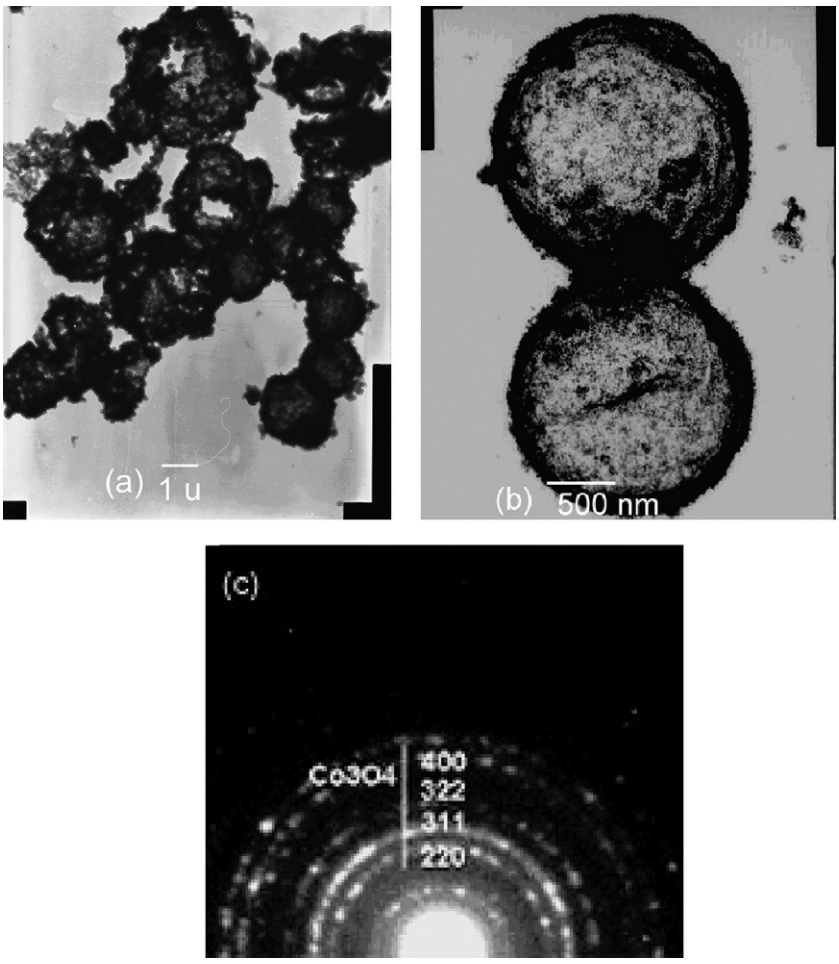

Fig. 3. TEM micrographs and electron diffraction (ED) patterns of hollow Co_3O_4 microspheres (HCMs): (a) low resolution; (b) high resolution; (c) ED.

more CO_2 molecules were formed. As a result, the CL intensity is stronger. The activity and CL represent the same process. It is reasonable that CL spectra can be used to quantitatively evaluate a given catalytic reaction. Fig. 7 shows the CL spectra of HCMs and SCPs. The CL intensity of HCMs is higher than that of SCPs (7×10^4 vs. 4.5×10^4), indicating that more CO molecules were oxidized into CO_2 molecules. The results may mean that HCMs had a higher catalytic activity for CO oxidation than SCPs. The catalytic activity for CO oxidation over the sample was further evaluated.

3.3. The reaction activity for CO oxidation over the catalysts

Fig. 8 shows the activities for CO oxidation over the samples. T_{10}, T_{50}, and T_{90} of HCMs were 135, 175 and 230 °C, respectively.

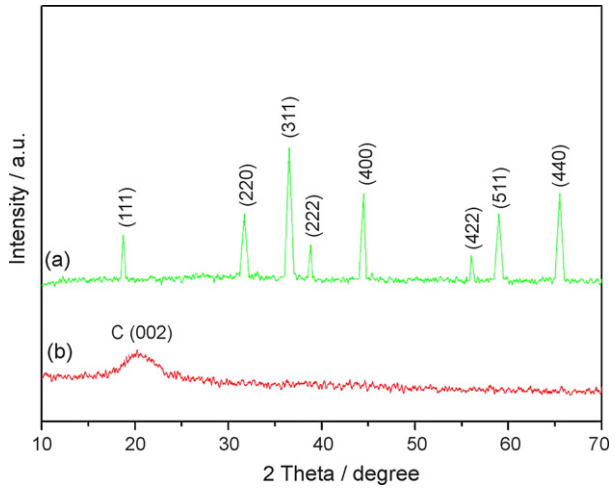

Fig. 4. XRD patterns of the samples: (a) carbonaceous microspheres (CMs); (b) hollow Co_3O_4 microspheres (HCMs).

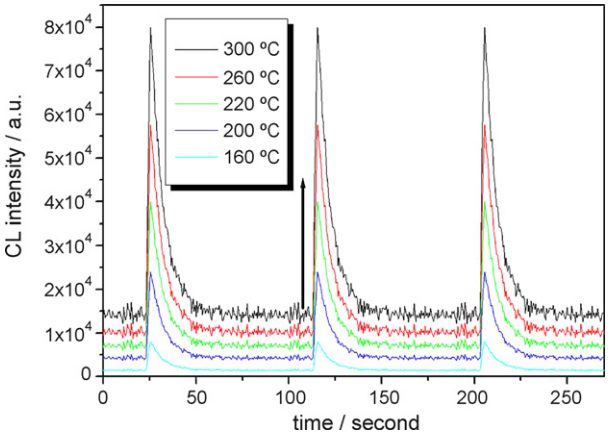

Fig. 5. The temperature dependent CL intensity of HCMs: $T = 300$ °C, F (flowing rate of gas) = 200 mL min^{-1}; C (CO concentration) = 200 μg mL^{-1}, λ_{filter} (wave number of filter) = 640 nm.

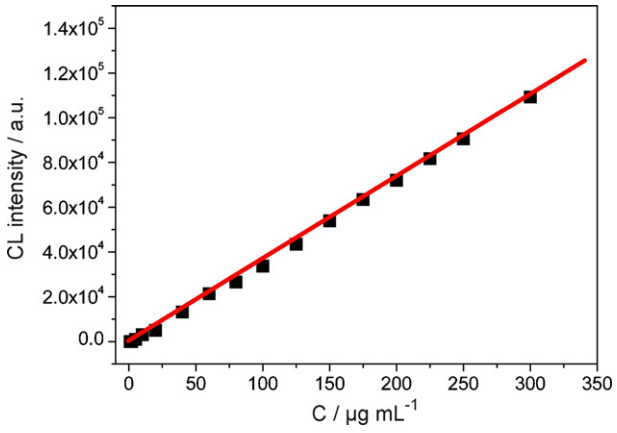

Fig. 6. The CO concentration (C)-dependent CL intensity of hollow Co_3O_4 microspheres (HCMs): T = 300 °C, F = 200 mL min^{-1}, λ_{filter} = 640 nm.

HCMs had a higher activity than the SCPs (T_{10}, T_{50} and T_{90}: 155, 200 and 270 °C), which is well consistent with their CL order. The textural properties of HCMs were characterized by N_2 adsorption isotherm (Table 2). The BET surface areas of HCMs and SCPs are 30.7 and 17.5 m^2 g^{-1}, respectively. The high BET area of HCMs is beneficial to adsorb molecules. Fig. S3 (see supporting material) shows CO-temperature-programmed desorption (TPD) profiles on

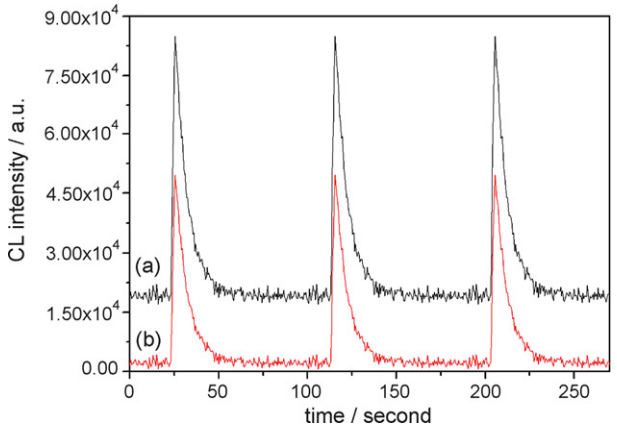

Fig. 7. The CL spectra of CO over (a) HCMs and (b) SCPs: T = 300 °C, F = 200 mL min^{-1}, λ_{filter} = 640 nm, C = 200 μg mL^{-1}.

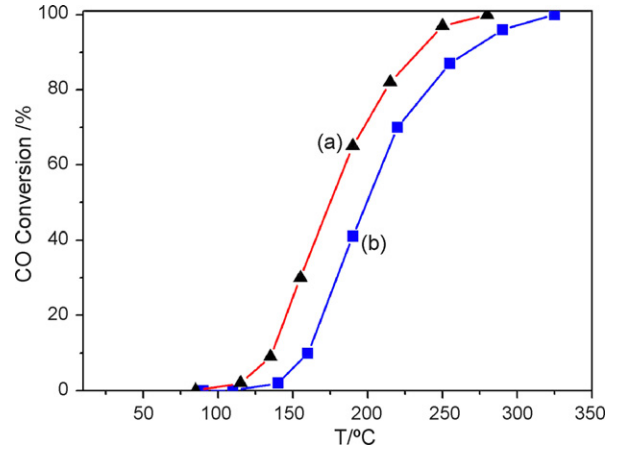

Fig. 8. The activities of CO oxidation over (a) hollow Co_3O_4 microspheres (HCMs) and (b) SCPs: 1 vol.% CO; 99 vol.% air, gas hourly space velocity (GHSV) = 12,000 h^{-1}.

Table 2
Surface areas, particle sizes and crystal sizes of hollow Co_3O_4 microspheres (HCMs) and solid Co_3O_4 particles (SCPs)

Sample	HCMs	SCPs
SA[a] (m^2 g^{-1})	30.7	17.5
Crystal[b] size (nm)	25.5	32.2
T_{10}[c] (°C)	135	155
T_{50}[c] (°C)	175	200
T_{90}[c] (°C)	230	270

[a] Surface area calculated by the BET method.
[b] Average crystal size calculated by Scherrer equation.
[c] T_{10}, T_{50}, and T_{90}, the temperatures at 10, 50 and 90% CO conversions, respectively.

the samples. In the range of 100–600 °C, 3 desorption peaks of CO can be observed over HCMs and SCPs. The adsorbed amounts of CO over both samples are significantly different (Table S1). The adsorbed amount on HCMs is higher than that on the latter.

The BET difference may be closely related to their different microstructures [29]. The BET surface area (30.7 m^2 g^{-1}) of HCMs is significantly larger than that (ca. 1.5 m^2 g^{-1}) of the hollow microspheres with an outer diameter of 5 μm and an inner diameter of 4.5 μm. The surface area of the latter is calculated on base of idea hollow microspheres (the theoretical density of Co_3O_4 is 6.056 g cm^{-3}). The calculation result further confirms that the increased surface area (29.2 m^2 g^{-1}) of HCMs may result from the pores in shells. The porous surface structures of the carbonaceous templates were passed onto the resultant shells after the removal of the templates. The increase of surface areas supports the formation of the porous shells, which resulted from the closely packing of Co_3O_4 nanocrystals. The high BET area of HCMs is beneficial to adsorb molecules, while the pores in the shells of the HCMs benefit the reactant molecules to get to the reactive sites of the catalysts. The chemical reactions can occur more easily, when the transport paths through which reactant molecules move in or out of the materials are included as an integral part of the porous structures.

3.4. Potential use of CL sensor for environmental combustible gases

Most importantly, the activity order of the catalysts is well consistent with that of CL intensity. This may indicate that CL mode can be an effective means to judge the catalyst activity, because the determination of CL spectra can be fulfilled within a few minutes. We have found that luminescent efficiencies and spectral shapes of the CL are dependent on the kinds of reactants and catalysts (Table S2, Figs. S6 and S7 of supporting material). Even if the same luminescent species could be produced from the different combustible gases on a given catalyst, the amounts of the generated luminescent species by different combustible gases are different. Therefore, the same nanomaterial exhibits different intensities of CL upon exposure to different gases. This enables us to discriminate the kind of combustible gas. The compounds within a given chemical class can be still discriminated effectively, because the mechanisms and rates of catalytic reactions are dependent on temperature, which leads to different luminescence efficiencies and spectral shapes [30]. Even if similar shape were recorded with the sensor for two gases at one temperature, they may be differentiated by different CL intensities at another temperature. We have fabricated a CL sensor (Fig. S8 of supporting material). The CL sensor system may be useful for analyzing various environmental toxic gases because of the linear characteristics of CL intensity as a function of gas concentration [29].

The CL properties on catalytic materials provide abundant optical information which motivates the fabrication of chemical sensor arrays. An intensive effort is currently devoted toward the develop-

ment of high-throughput screening approaches. The CL reaction is of practical importance for detecting environmental pollutants or selecting catalysts. The extensive researches are ongoing.

4. Conclusions

Compared with the SCPs, the HCMs showed a stronger CL intensity and a higher catalytic activity for CO oxidation, which was attributed to the hollow microstructure. The good correlation between CL and activity indicates that the CL mode is a facile and rapid means for the detection of environmentally deleterious gases and the selection of excellent catalysts from thousands of materials.

Acknowledgements

The authors gratefully acknowledge the research funding supported by National Basic Research Program of China (2007CB613303) and Chinese Postdoctoral Science Foundation (No. 20060390057).

Appendix A. Supplementary data

Supplementary data associated with this article can be found, in the online version at doi:10.1016/j.talanta.2008.05.011.

References

[1] M. Breysse, B. Claudel, L. Faure, M. Guenin, R.J.J. Williams, T.J. Wolkenstein, J. Catal. 45 (1976) 137.
[2] M.C. Daniel, D. Astruc, Chem. Rev. 104 (2004) 293.
[3] R. Elghanian, J.J. Storhoff, R.C. Mucic, R.L. Letsinger, C.A. Mirkin, Science 277 (1997) 1078.
[4] I.H. El-Sayed, X. Huang, M.A. El-Sayed, Nano Lett. 5 (2005) 829.
[5] A.M. Powe, K.A. Fletcher, N.N. St. Luce, M. Lowry, S. Neal, M.E. McCarroll, P.B. Oldham, L.B. McGown, I.M. Warner, Anal. Chem. 76 (2004) 4614.
[6] Y.F. Zhu, J. Shi, Z. Zhang, C. Zhang, X.R. Zhang, Anal. Chem. 74 (2002) 120.
[7] N.A. Rakow, K.S. Suslick, Nature 406 (2000) 710.
[8] M. Nakagawa, T. Okabayashi, T. Fujimoto, K. Utsunomiya, I. Yamamoto, T. Wada, Y. Yamashita, N. Yamashita, Sens. Actuators B 51 (1998) 159.
[9] T. Okabayashi, T. Fujimoto, I. Yamamoto, K. Utsunomiya, T. Wada, Y. Yamashita, N. Yamashita, M. Nakagawa, Sens. Actuators B 64 (2000) 54.
[10] Z.Y. Zhang, C. Zhang, X.R. Zhang, Analyst 127 (2002) 792.
[11] J.J. Shi, J.J. Li, Y.F. Zhu, W. Fan, X.R. Zhang, Anal. Chim. Acta 466 (2002) 69.
[12] Z.M. Rao, J.J. Shi, X.R. Zhang, Acta Chim. Sin. 60 (2002) 1668.
[13] T. Corralles, C. Peinado, N.S. Allen, M. Edge, G. Sandoval, F.J. Catalina, Photochem. Photobiol. A 156 (2003) 151.
[14] F. Caruso, R.A. Caruso, Science 282 (1998) 1111.
[15] T. He, D. Chen, X. Jiao, Y. Xu, Y. Gu, Langmuir 20 (2004) 8404.
[16] B. Liu, H. Zeng, Small 1 (2005) 566.
[17] Q. Ye, Q. Gao, X.R. Zhang, B.Q. Xu, Acta Chim. Sin. 64 (2006) 751.
[18] X. Sun, J. Liu, Y. Li, Chem. Eur. J. 12 (2006) 2039.
[19] Y.F. Shen, P.R. Zerger, N.R. DeGuzman, L.S. Suib, L. McCurdy, I.D. Potter, C.L. O'Young, Science 260 (1993) 511.
[20] X. Sun, Y. Li, Angew. Chem. Int. Ed. 43 (2004) 597.
[21] V.K. Lamer, Ind. Eng. Chem. 44 (1952) 1270.
[22] H. Qian, G. Lin, Y. Zhang, P. Gunawan, R. Xu, Nanotechnol. 18 (2007) 355602.
[23] J. Huang, T. Kunitake, J. Am. Chem. Soc. 125 (2003) 11834.
[24] S. Chen, H. Zeng, Carbon 41 (2003) 1265.
[25] R. Fu, H. Zeng, Y. Lu, Carbon 31 (1993) 1089.
[26] M. Nakagawa, N. Yamashita, Springer Ser. Chem. Sens. Biosens. 3 (2005) 93.
[27] X. Wang, N. Na, S. Zhang, Y. Wu, X. Zhang, J. Am. Chem. Soc. 129 (2007) 6062.
[28] X.Y. Huang, J.C. Ren, Trends Anal. Chem. 25 (2006) 155.
[29] G.S. Chai, S.B. Yoon, J. Ho Kim, J.S. Yu, Chem. Commun. 11 (2004) 2766.
[30] N. Na, S. Zhang, S. Wang, X. Zhang, J. Am. Chem. Soc. 128 (2006) 14420.